APPLICABILITY OF THE 3D TRANSPORT CODE TORT TO THE SHIELDING ANALYSIS OF THE REACTOR CAVITY SHIELDING FLOOR IN THE PROTOTYPE FBR MONJU

Kenji SASAKI, Shin USAMI
Japan Nuclear Cycle Development Institute
esasaki@t-hq.jnc.go.jp; eusami@t-hq.jnc.go.jp

Takako SHIRAKI, Keiko TADA, Hitoshi YOKOBORI
Advanced Reactor Technology Co., Ltd.
shiraki@artech.co.jp; tada@artech.co.jp; yokobori@artech.co.jp

ABSTRACT

During the start-up tests of the prototype FBR Monju reaction rates inside the reactor vessel (RV) were measured in the shielding measurement program and in future it is planned to measure reaction rates outside RV. The purpose of these measurements is to obtain basic data for shielding design including the incident fluxes at the reactor head access area and the primary heat transport system cells. These data are essential to evaluate the shielding design accuracy around the reactor. Two-dimensional discrete ordinates transport codes such as DOT3.5[(1)] and DORT[(2)] have been widely used for shielding design, but the shielding floor inside the reactor cavity has three-dimensional structure containing various penetrations and shielding defects. The shape of the reactor cavity wall is hexagonal because of the three-loop symmetry. Therefore in order to improve the shielding design accuracy the three-dimensional discrete ordinates transport code, TORT[(3)], was employed for analysis of the line of the primary sodium overflow system and the primary coolant inlet piping of the shielding floor. As a result the applicability of the code was confirmed, and the amounts of streaming through the penetrations and the shielding defects were evaluated using more realistic three-dimensional calculation models. The results were compared with the design calculation to confirm that the design values with the two-dimensional models are sufficiently conservative.

I INTRODUCTION

The prototype fast breeder reactor MONJU has a three-dimensionally shaped shielding structure containing various penetrations and shielding defects in the shielding floor of the reactor cavity. The purposes of this study are to confirm the applicability of the three-dimensional discrete ordinates transport code, TORT, for complicated FBR systems and to evaluate the streaming amounts through the penetrations and the shielding defects of the shielding floor with more realistic calculational models. The structure of Monju is shown in **Fig.1**.

There are two main paths of the neutrons generated in the core. One goes from the core to the reactor vessel (RV) radially and then goes upward to the entrance of the primary heat transport system cells, and the other goes from the core to the pedestal axially. In order to shield these neutrons, there are a shielding floor and various additional shields of three-dimensional shapes with various penetrations and shielding defects, and the shape of the reactor cavity wall is hexagonal. This study reports the results of the analyses upon the line of the primary sodium overflow system and the primary coolant inlet piping of the shielding floor using the three-dimensional discrete ordinates transport code, TORT. The points of interest in this study are at the bottom of the pedestal and the entrance to the first penetration to the primary heat transport system cell and the dose rates were evaluated at these points. The amounts of the neutron streaming through the line of the primary sodium overflow system and the primary coolant inlet piping were calculated, because they were considered to have larger effects to the points of interest.

II STRUCTURE OF THE SHIELDING FLOOR

The main shielding structures around the reactor core in Monju are the reactor cavity wall in the radial direction, and the shielding plug and the pedestal in the upper axial direction. The shielding floor is provided in the reactor cavity to reinforce shielding for the reactor head access area (RHAA) and the primary heat transport system cells. The reactor cavity wall is of concrete-filled steel structure. The shielding plug is constructed of multiple layers of stainless steel, carbon steel and polyethylene. The pedestal has a serpentine concrete-filled steel structure, and forms part of RHAA around the shielding plug. The structure of the shielding floor is shown in **Fig. 2**. The shielding floor is constructed of the reactor cavity shielding floor (RCSF), shielding on RCSF, shielding around primary piping (SPP), shielding on the guard vessel (GV) flange and shielding on the reactor vessel conical part (SRVC). The reactor cavity shielding floor consists of a concrete-filled steel structure of 110 cm thickness and has the 120° symmetry. The thickness of SPP is 52 cm. It is installed to reinforce shielding for the defects due to the penetration of the primary piping and the ISI guide tube and is located at the 0°, 120° and 240°direction. There is a

gap between RCSF and SPP as shown in **Fig. 3**. There are various shielding defects, such as the line of the primary sodium overflow system and the RV main body ISI guide tubes in the shielding of RCSF.

III CALCULATION METHOD

1 Outline of calculation and calculation cases

The calculations were performed in accordance with the FBR shielding analysis method and the boot strap technique with the two-dimensional discrete ordinates transport code. This method is shown in **Fig. 4**. The 100 neutron group effective macroscopic-cross sections were calculated by using the shielding constant calculation code RADHEAT-V3[(4)(5)] with the infinite dilution cross-section library JSD-J2[(6)] based on the nuclear data file JENDL-2[(7)]. These macroscopic effective cross-sections were collapsed into 21 neutron groups by the one-dimensional transport calculation code ANISN-W[(8)]. The neutron flux distributions were calculated with the three-dimensional calculation code, TORT, instead of a two-dimensional calculation code. The calculation flow is shown in **Fig.5**.

At first, a two-dimensional calculation was performed to obtain angular fluxes at 375.5 cm from the core central plane. These angular fluxes were used as the bottom source of subsequent three-dimensional calculations. The calculation area was radially from the core to the reactor cavity wall and axially from the lower part of the floor of the reactor cavity to the pedestal in RZ geometry. The model is shown in **Fig.6**. In this model RCSF and SPP were modeled as a single ring shaped structure consisting of 49.6 cm thick concrete with a 1.2 cm thick liner because RCSF and SPP are made of the same material and constitute shielding in θ-direction as shown in Fig.3. Therefore in the two-dimensional calculation the gap between RCSF and SPP were not taken into account, neither the penetration nor the shielding defects in the shielding floor. This model is to be called bulk model of the two-dimensional calculation. The calculation condition is shown in **Table 1**. The fission sources in the core and blanket were calculated with a diffusion code.

Three-dimensional calculations were performed in RθZ geometry. The calculation condition is shown in **Table 2**. The calculation area was radially from RV to the reactor cavity wall and axially from the lower surface of SPP to the pedestal. Monju core has 120° symmetry in the θ-direction, therefore the calculation was performed for the sector between $60° \leq \theta \leq 180°$ with the periodic boundary condition. The boundary angular fluxes of the TORT calculations were the angular fluxes under SPP calculated by DOT 3.5. The Sn calculation was carried out with asymmetric S140. Writing the direction cosine of the angular vector with respect to the Z-axis as η , there are 10 levels of η and 15 angular points per octant. The order of scattering

anisotropy was P3. The number of the spatial meshes (R•θ•Z) were 90•80•82. The spatial mesh intervals were smaller than 10 cm in R and Z directions, and the θ intervals were 1.5°. The order of Sn calculation and the order of scattering anisotropy are the same as in the design calculation. The intervals of the spatial meshes are chosen so that the total memory size is within 1 GB considering the calculation machine capacity, but they are nearly the same as in the design calculation. It was confirmed that this order of Sn and these spatial mesh intervals give a factor 2 underestimation using DOT3.5. This factor is not small from the design calculation improvement point, but the order of Sn, the order of scattering anisotropy and the spatial mesh intervals were restricted due to the computer capacity. Since the order of Sn and the mesh intervals are approximately same for the two-dimensional and the three-dimensional calculations with the same kind of the computer codes, only the ratios of the calculated results are evaluated to minimize the error coming from these calculation parameters. Three cases of calculation were performed: (1) Bulk base model, (2)Primary coolant inlet piping model, and (3) Line of the primary sodium overflow system model. The models of (2) and (3) are the streaming models.

(1) Bulk base model

In this model it is assumed that there is no streaming through penetrations and shielding defects in the shielding floor except through the gap between RCSF and SPP. It is called bulk base model because it is taken as a reference for streaming evaluation. The calculation model is shown in **Fig. 7**.

(2) Primary coolant inlet piping model

This model is directed to the RCSF penetration by the primary coolant inlet piping. The primary coolant inlet piping is taken into account to the bulk model to evaluate streaming, and is called primary coolant inlet piping model. The primary coolant inlet piping of 24B diameter penetrates through the φ101 cm opening of RCSF. A ring shaped B_4C collar is installed at the bottom of the penetration to reinforce shielding. The calculation model is shown in **Fig. 8**.

(3) Line of the primary sodium overflow system model

This model is directed to evaluation of streaming through the shielding defect on RCSF by the line of the primary sodium overflow system. The line of the primary sodium overflow system was introduced to the bulk model, and is called line of the primary sodium overflow system model. There is the line of the primary sodium overflow system of 4B diameter at θ=85° making about a 7000 cm^2 shielding defect to the shielding on the GV flange. Additional serpentine concrete is installed on the shielding defect to reinforce shielding. The calculation model is shown in **Fig. 9**.

(4) Evaluation of streaming amounts

Neutron streaming coefficients are defined as the ratio of the streaming calculation to the bulk calculation.

2 Preparation of boundary angular flux

The boundary angular fluxes to start the three-dimensional calculations were obtained from the two-dimensional RZ calculation of DOT3.5. The angular fluxes of DOT3.5 at Z=375.5 cm from the core central plane were transformed to the boundary fluxes in RθZ geometry. Since the calculation area of TORT was radially from RV to the reactor cavity wall as shown in **Fig. 6**, only the upward angular fluxes by DOT 3.5 in this area were used. In addition the order of Sn of the three-dimensional calculation was different from that of the two-dimensional calculation, and the boundary mesh locations of each area (R<GV Flange, GV Flange<R<Reactor cavity wall, R>Reactor cavity wall) change at each θ mesh point because the bottom interface of the TORT calculation has a shape as shown in **Fig. 10**. Therefore the angular fluxes of DOT3.5 were transformed as follows.

(1) Processing method of R mesh boundary

The angular fluxes of DOT3.5 were interpolated according to the distance from the core center to obtain the TORT boundary fluxes. In doing this the angular fluxes were normalized so that the leakage per unit area of TORT was the same as that of DOT3.5.

(2) Processing method of angular quadrature

Denoting the direction cosines of the angular vectors with respect to the rectangular coordinate axes as μ, η and ξ, the boundary angular flux of TORT, $\psi_t(\mu_t, \eta_t, \xi_t)$, is defined as $\psi_t(\mu_t, \eta_t, \xi_t)=\psi_d(\mu_d, \eta_d, \xi_d)$ such that

$|1-(\mu_d \bullet \mu_t+\eta_d \bullet \eta_t + \xi_d \bullet \xi_t)|$ ~ minimum

where $\psi_d(\mu_d, \eta_d, \xi_d)$ is the boundary angular flux obtained by DOT3.5.

In addition the boundary fluxes of TORT are normalized so that the total leakage in each area (R<GV Flange, GV Flange<R<Reactor cavity wall, R>Reactor cavity wall) is the same as that of DOT3.5.

The left boundary condition was taken to be void, because the influence of the incident fluxes from the left side is found to be small as shown in the following. The two-dimensional bulk calculation results were compared with two-dimensional calculation results where the bulk results were given as the inner boundary source at the corresponding left boundary of TORT. As a result it became clear that the neutrons coming from the left boundary effect the neutron flux approximately less than 10 % at the point of interest.

IV CALCULATION RESULT

1 Bulk base model

The total neutron flux distribution from the bulk base model is shown in **Fig. 11**. The result clearly shows the gap streaming between RCSF and SPP. This streaming could not be observed until the three-dimensional model was introduced, because the gap could not be modeled properly in two-dimensional calculations.

2 Primary coolant inlet piping model

The total neutron flux distribution from the primary coolant inlet piping model is shown in **Fig. 12**. The neutron streaming coefficients (primary coolant inlet piping model / bulk base model) are shown in **Table3**, and are 1.2~2.4 at the bottom of the pedestal and 1.7~1.8 at the entrance to the first penetration of the primary heat transport system cell.

3 Line of the primary sodium overflow system model

The total neutron flux distribution from the line of the primary sodium overflow system model is shown in **Fig. 13**. The neutron streaming coefficients (line of the primary sodium overflow system model / bulk base model) are shown in **Table 4**. The neutron streaming coefficients are 1.0~1.3 at the bottom of the pedestal, and 1.1 at the entrance to the first penetration of the primary heat transport system cell.

V DISCUSSION AND CONCLUSION

1 Applicability

The calculated values of the bulk base model of TORT were compared with the calculated values of the bulk model of DOT3.5 in order to check the validity of the TORT calculation. The results are shown in **Table 5**. The ratios of total fluxes (TORT /DOT3.5) are 1.0~1.6 at the bottom of the pedestal, and 0.9~1.1 at the entrance to the first penetration of the primary heat transport system cell. The maximum difference between the values of TORT and DOT3.5 is 60%. The TORT fluxes tend to be larger than the DOT3.5 fluxes. The reason is that the three-dimensional calculation was able to model the gap between SPP and RCSF taking the neutron streaming into account more correctly.

The neutron streaming coefficients around the line of the primary sodium overflow system and the primary coolant inlet piping at the bottom of the pedestal are larger than those at the entrance to the first penetration of the primary heat transport piping cell because most of the neutrons stream to the upper direction through the penetrations and the shielding defects. The neutron streaming coefficients around the line of the primary sodium overflow system are

smaller than those around the primary coolant inlet piping because of the additional shielding to the defect due to the line of the primary sodium overflow system.
From these the calculation results of TORT show a qualitatively correct tendency, thus confirming its applicability to a design evaluation. The CPU time was within 5500 minutes on EWS Ultra SPARC Solaris 2.5($6.2 \cdot 10^{-8}$minutes/1unit).

2 Comparison between the three-dimensional calculation and the design calculation

The three-dimensional values and the design calculation values were compared with respect to neutron streaming at the primary coolant inlet piping. The design calculations were carried out with a bulk model assuming that there are no penetration nor shielding defects in the shielding floor and with a primary coolant inlet piping model including the RCSF penetration by the primary coolant inlet piping with DOT3.5 as is shown in **Fig.14**. An RZ model centered at the primary coolant inlet pipe was used with asymmetric S59 and P3. The incident fluxes were given at the lower part of SPP. The neutron streaming coefficients are shown in **Table 6**. It is confirmed that the neutron streaming coefficients for the design calculations and the three-dimensional calculation agree sufficiently at the points of interest. As a result, the evaluation model used in the design can be considered well appropriate for the maximum flux evaluation at the points of interest. However, TORT makes it possible to evaluate the flux distribution in the θ-direction which can not be obtained with the two-dimensional models employed in the design calculation.

In future the application of the three-dimensional code is indispensable for more detailed evaluation. In this study the order of Sn and the number of spatial meshes are not fine enough due to the restriction of the computer. With the advancement of the computer technology calculation of the order of tens of GB capacity is becoming possible and we plan to perform much finer analysis.

VI REFERENCE

(1) R.S.I.C: “DOT3.5 Two-Dimensional Discrete Ordinates Transport Code”, (RSIC Computer Code Collection) CCC-276 (1975).
(2) Oak Ridge National Laboratory : “RSIC Computer Code Collection, DORT Two-Dimensional Discrete Ordinates Transport Code”, CCC-484 (1989).
(3) Rhoades, W.A., Childs, R.L.: “Three Dimensional Discrete Ordinates Neutron/Photon Transport Code”, ORNL-6268 (1987).
(4) S.Miyasaka, et al. : “Code System for the Radiation-heating Analysis of a Nuclear Reactor, RADHEAT”, JAERI-M5794 (1974).

(5) K.Koyama, et al. : “RADHEAT-V3, A Code System for Generating Coupled Neutron and Gamma-ray Group Constants and Analyzing Radiation Transport”, JAERI-M7155 (1977).
(6) M.Takemura, et al: 1987 Fall Mtg. of the Atomic Energy Society of Japan, A61, Oct. (1987).
(7) T.Nakagawa, “Summary of JENDL-2 General Purpose File”, JAERI-M 84-103 (1984).
(8) W.W Engle Jr. : “A User Manual for ANISN: A One-Dimensional Discrete Ordinates Transport Code with Anisotropic Scattering”, K-1963 (1967).

Table 1 DOT3.5 Code Calculation Conditions

Item	Condition
Code	DOT3.5
Cross Section	JENDL2
Model	RZ
Calculation Area	Core<R<Reactor Cavity Shielding Wall
	Floor of the Reactor Cavity<Z<Pedestal
No. of Mesh	IM=233,JM=355
Boundary Condition	Left:reflected, Right:void
	Bottom:void, Top:void
No. of Energy Groups	Neutron:21
Order of Scattering Anisotropy	P3
No. of Angular Directions	S48
Flux Convergence Criterion	<0.01

Table 2 TORT Code Calculation Conditions

Item	Condition
Code	TORT
Cross Section	JENDL2
Model	R θ Z
Calculation Area	Reactor Vessel<R<Reactor Cavity Wall
	60 < θ (degree) < 180
	Reactor Cavity Shielding Floor<Z<Pedestal
No. of Mesh	IM=91,JM=80,KM=82
Boundary Condition	Left:void, Right:void
	Inside:periodic, Outside:periodic
	Bottom:boundary source, Top:void
No. of Energy Groups	Neutron:21
Order of Scattering Anisotropy	P3
No. of Angular Directions	S140
Flux Convergence Criterion	<0.01

Table3 Neutron Streaming Coefficients around the Line of the Primary Coolant Inlet Piping

Neutron Streaming Coefficients	Bottom of the Pedestal	Entrance to the first penetration of the primary heat transport system cell
Fast Flux	1.2 ~ 4.9	2.1 ~ 2.4
Intermediate Flux	1.3 ~ 4.4	2.6 ~ 2.7
Thermal Flux	1.2 ~ 1.7	1.5 ~ 1.6
Total Flux	1.2 ~ 2.4	1.7 ~ 1.8

Table4 Neutron Streaming Coefficients around the Line of the Primary Sodium Overflow System

Neutron Streaming Coefficients	Bottom of the Pedestal	Entrance to the first penetration of the primary heat transport system cell
Fast Flux	1.0 ~ 1.9	1.1 ~ 1.2
Intermediate Flux	1.1 ~ 1.7	1.1 ~ 1.2
Thermal Flux	1.0 ~ 1.1	1.1
Total Flux	1.0 ~ 1.3	1.1

Table5 Comparison with DOT3.5 and TORT(Bulk Base Model)

TORT/DOT3.5	Bottom of the Pedestal	Entrance to the first penetration of the primary heat transport system cell
Fast Flux	1.2 ~ 2.2	0.6 ~ 0.7
Intermediate Flux	0.7 ~ 1.2	0.4 ~ 0.5
Thermal Flux	1.2 ~ 1.9	1.3 ~ 1.5
Total Flux	1.0 ~ 1.6	0.9 ~ 1.1

Table6 Neutron Streaming Cosfficients through the Primary Coolant Inlet Piping

Neutron Streaming Coefficients	Bottom of the Pedestal	Entrance to the first penetration of the primary heat transport system cell
	Flux (E>10keV)	Total Flux
Design	1.5	1.2
TORT	1.2 ~ 2.4	1.7 ~ 1.8

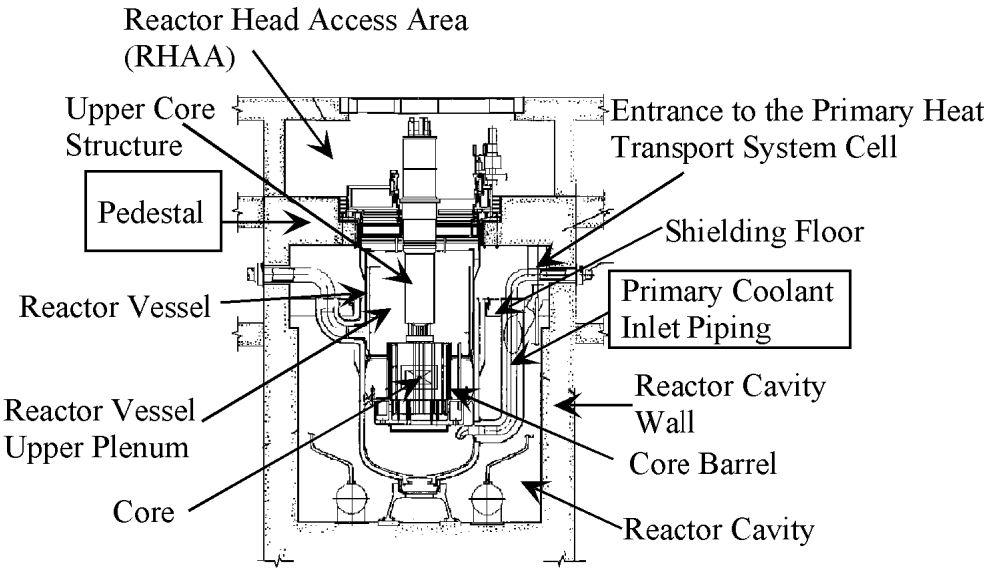

Fig.1 Structure of Monju

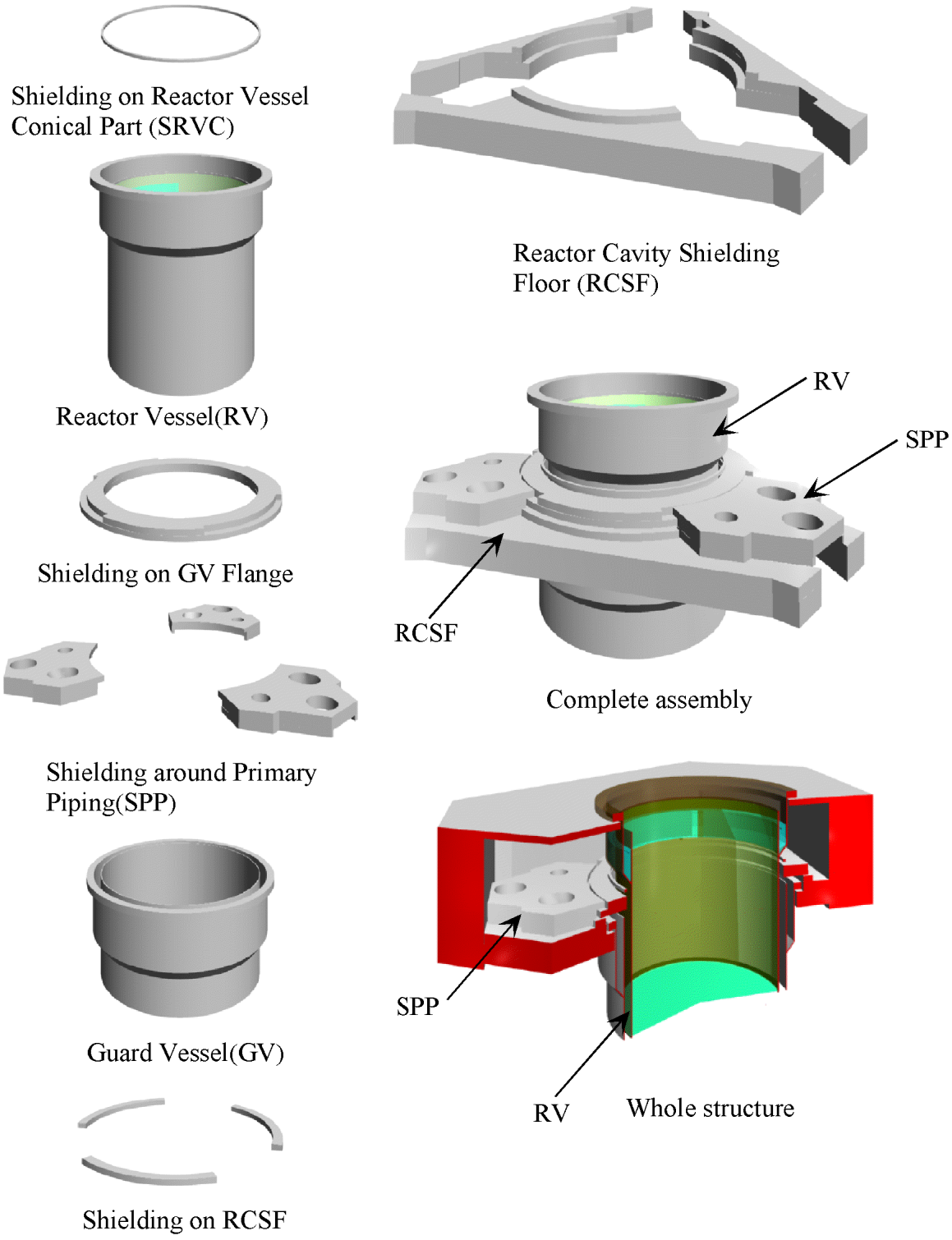

Fig2. Structure of the Shielding Floor

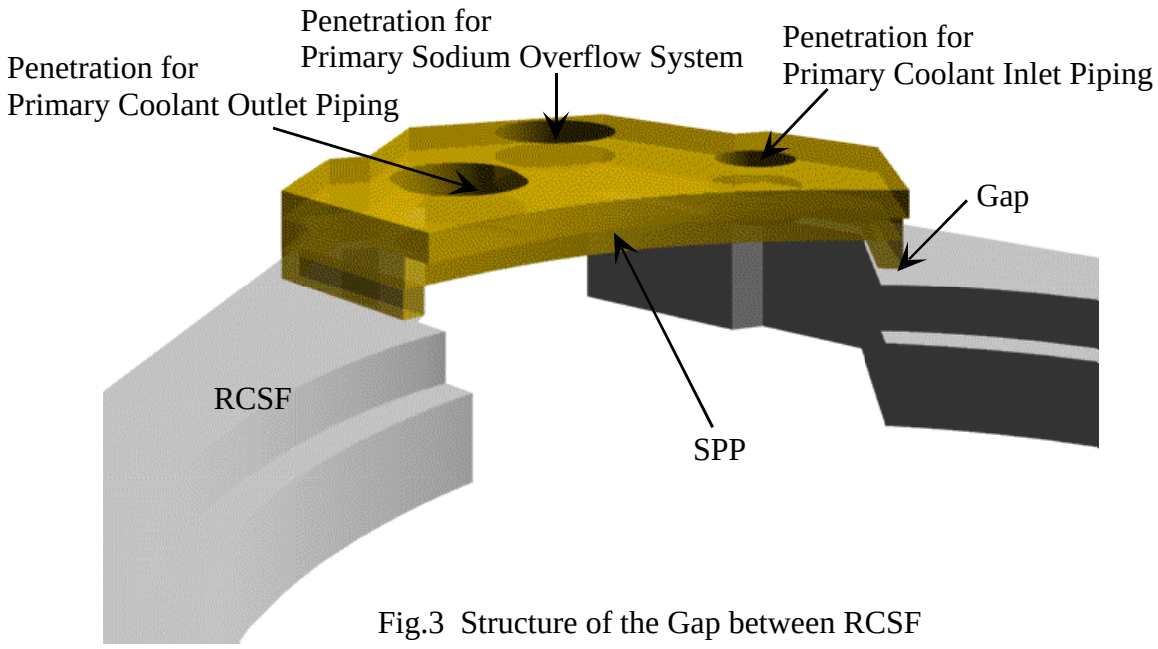

Fig.3 Structure of the Gap between RCSF

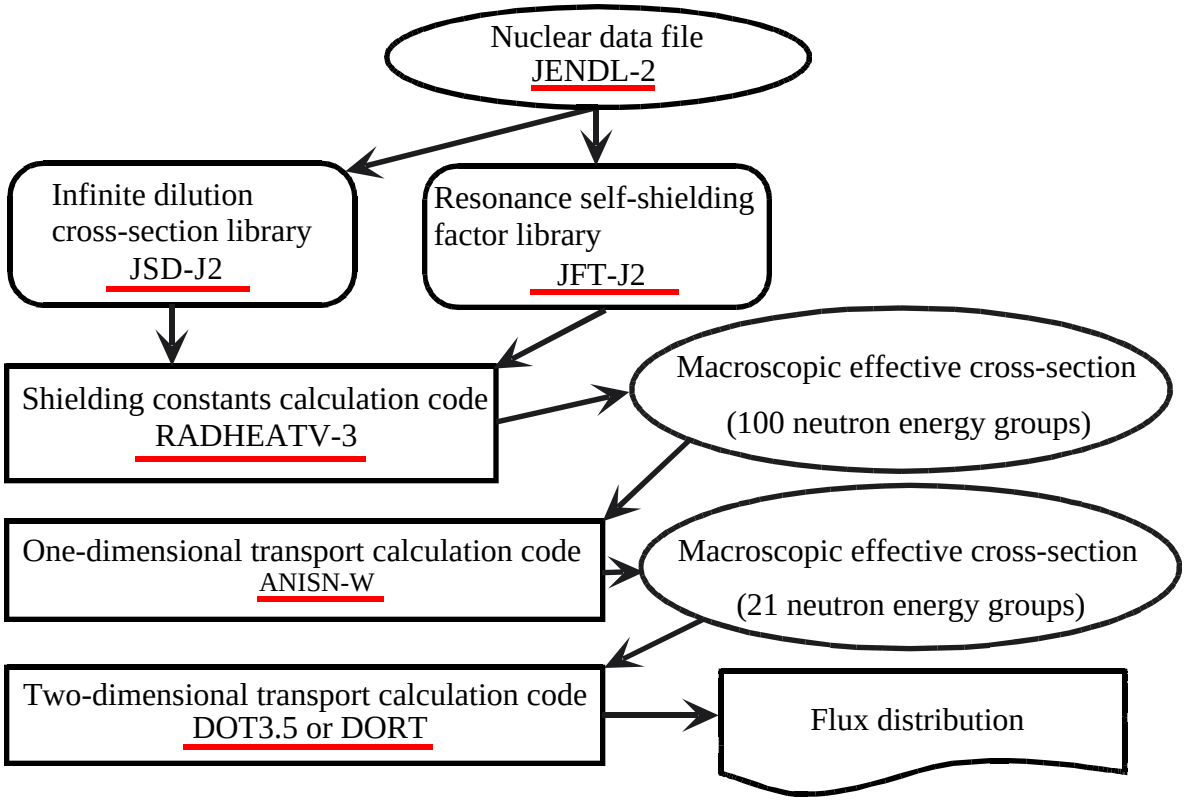

Fig.4 FBR Shielding Analysis Method

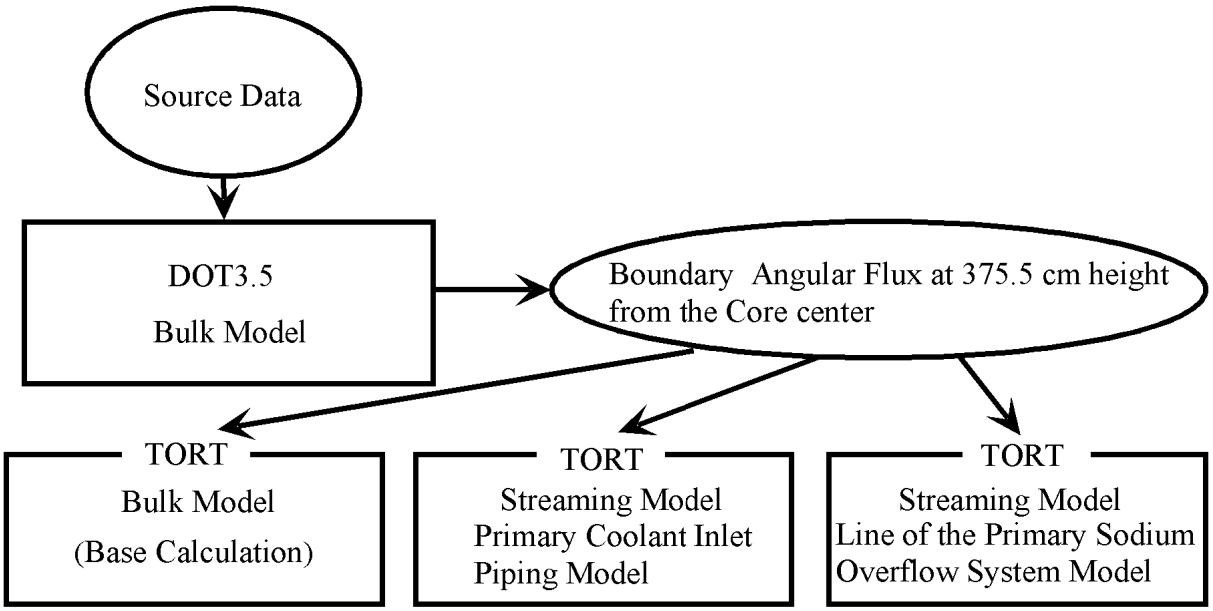

Fig.5 Calculation Flow

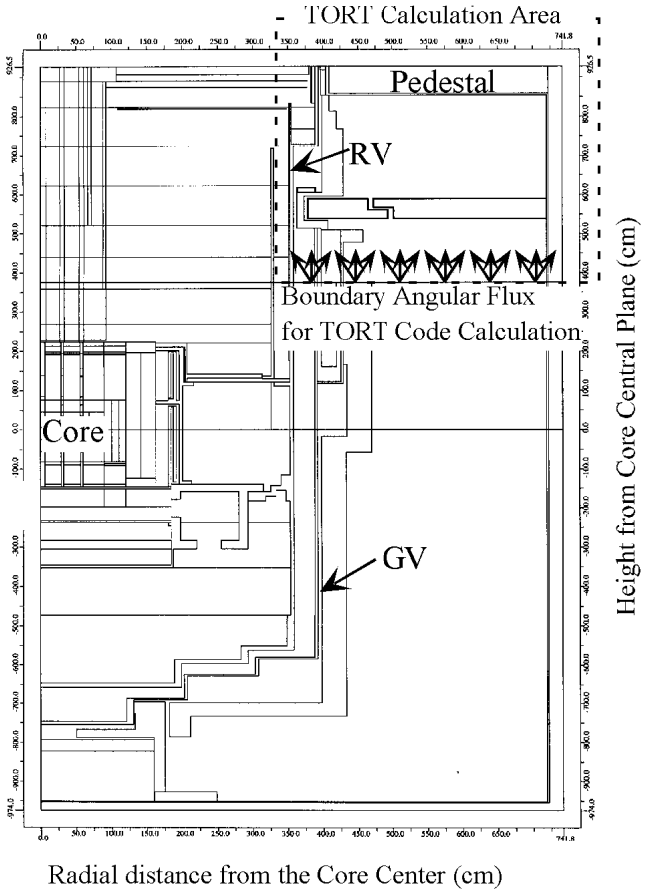

Fig.6 DOT3.5 Calculation Model

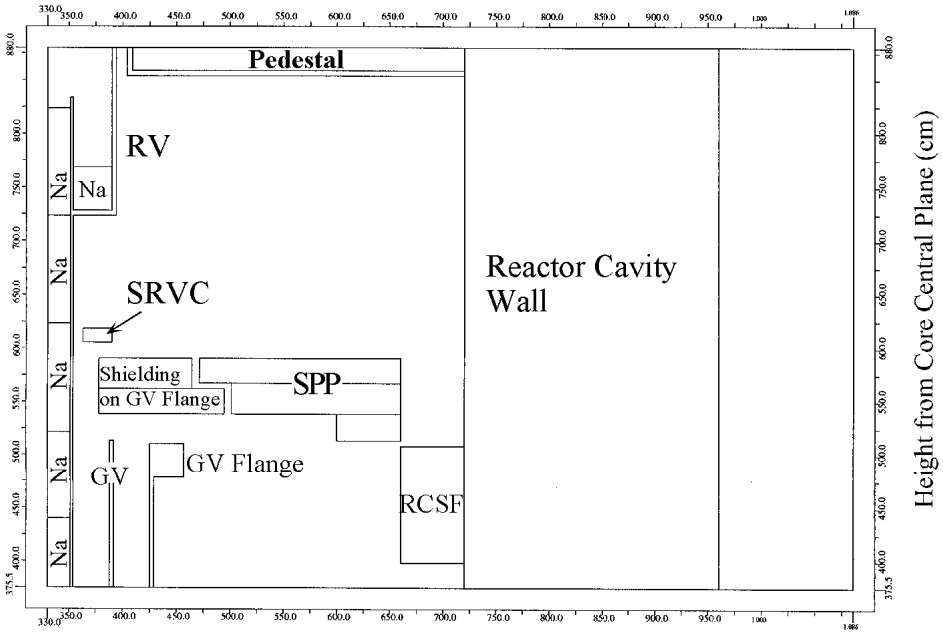

θ=145°

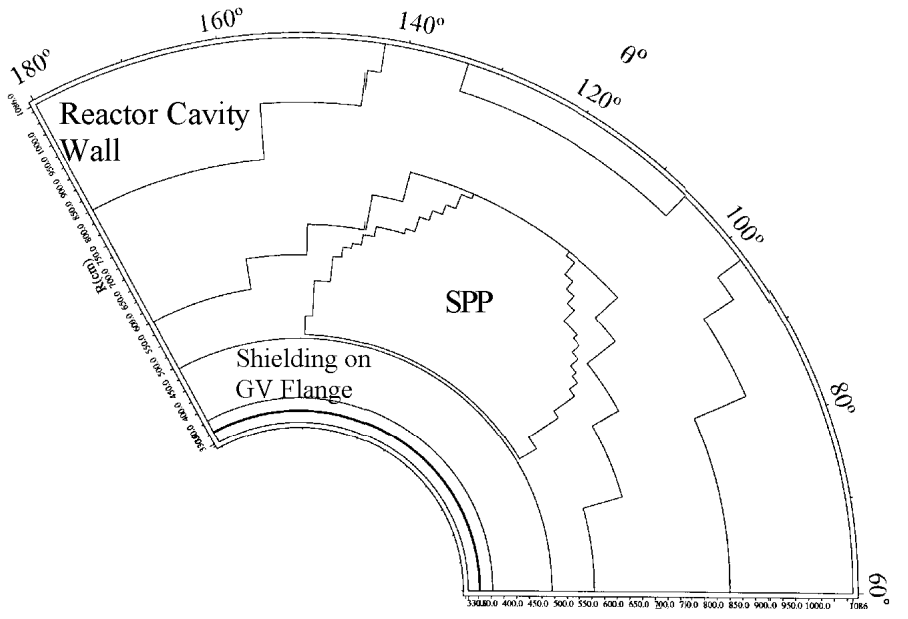

Z=550cm

Fig.7 Bulk Base Model

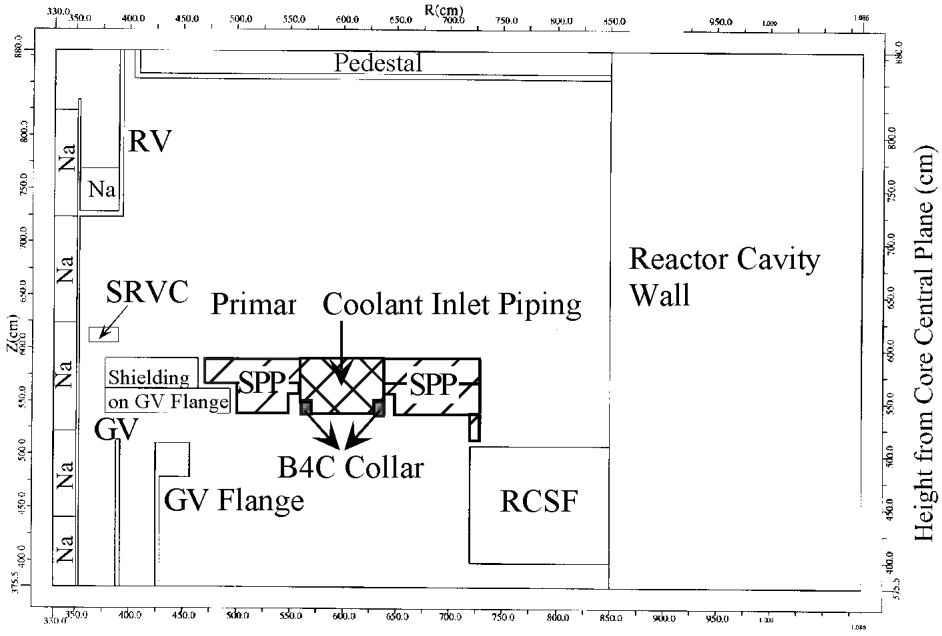

θ=145°

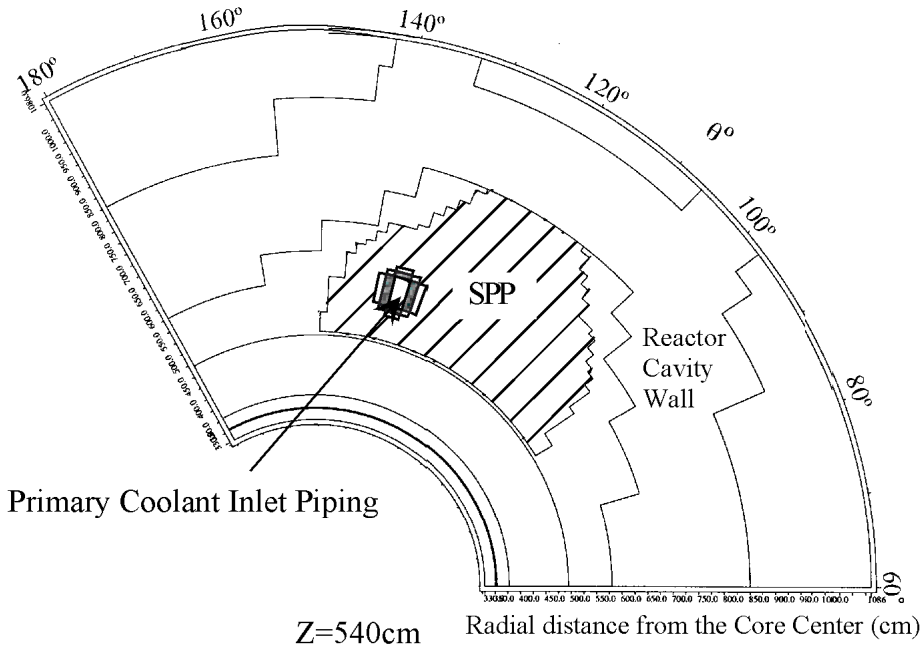

Fig.8 Primary Coolant Inlet Piping Model

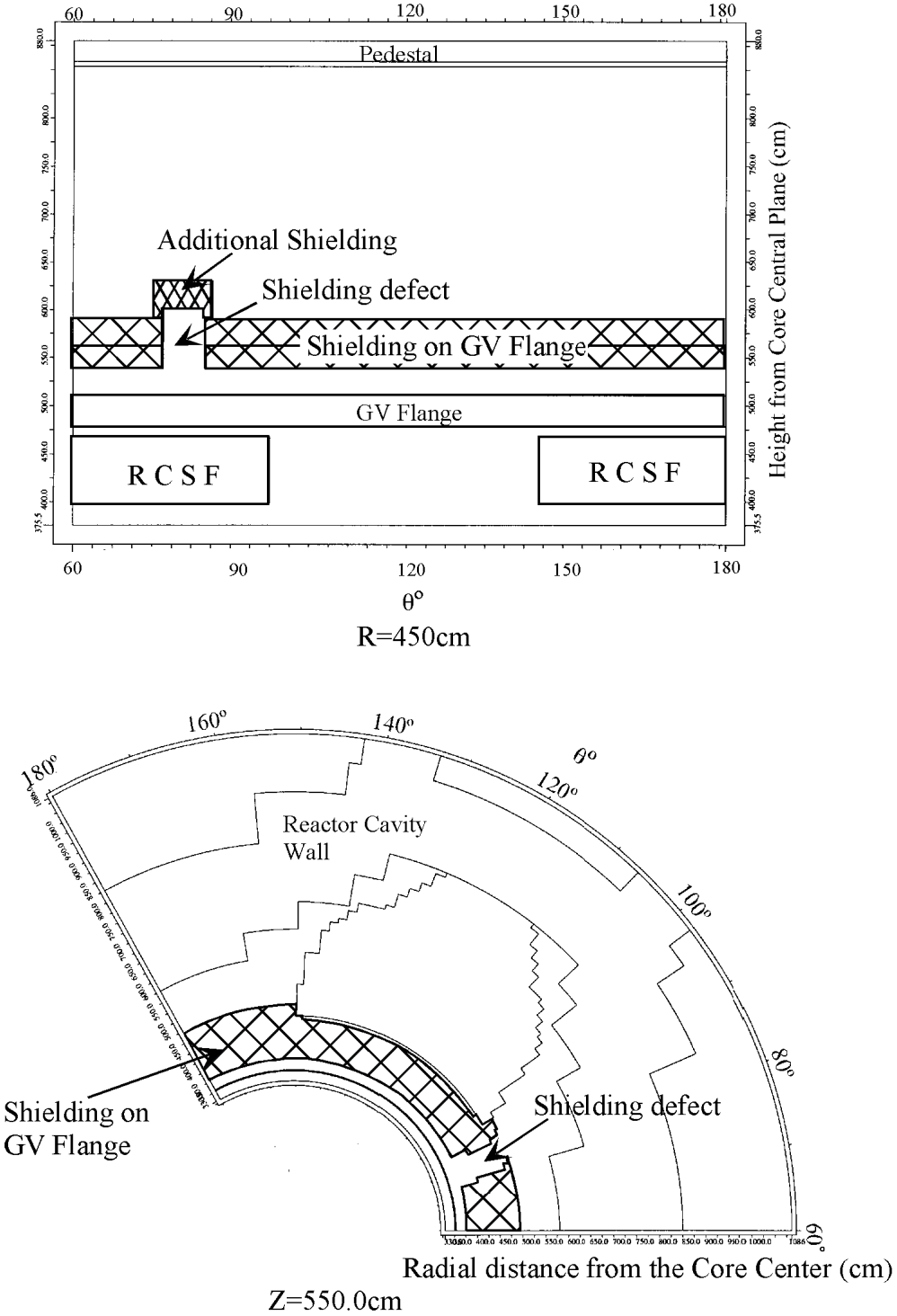

Fig.9 Line of the Primary Sodium Overflow System Model

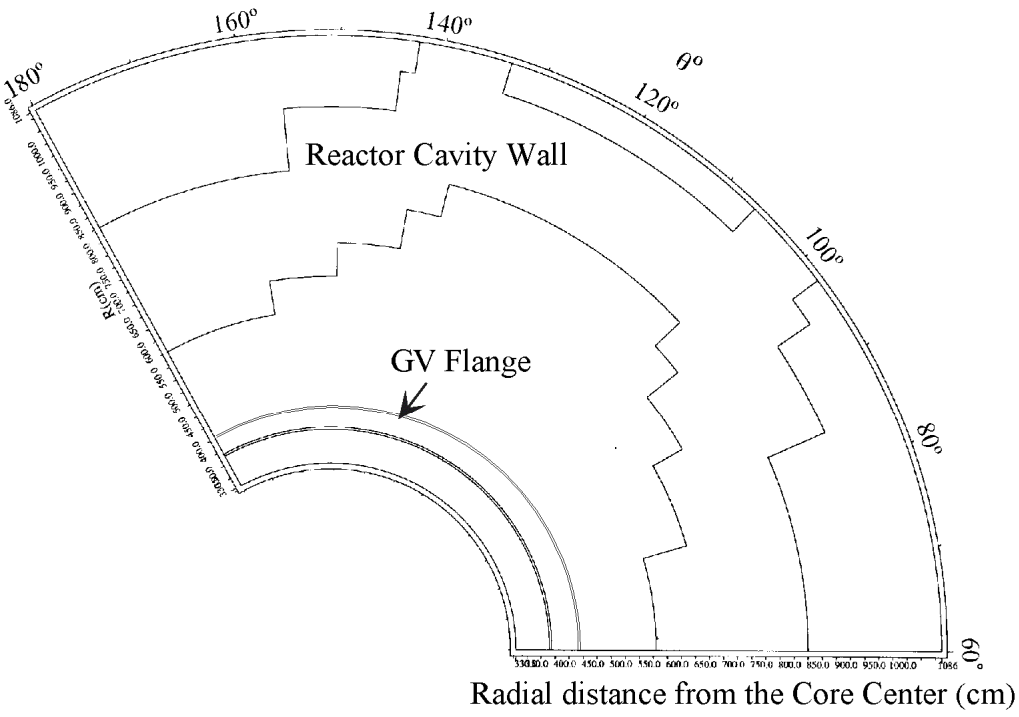

Z=375.5cm

Fig.10 Bottom Plane of the TORT Model

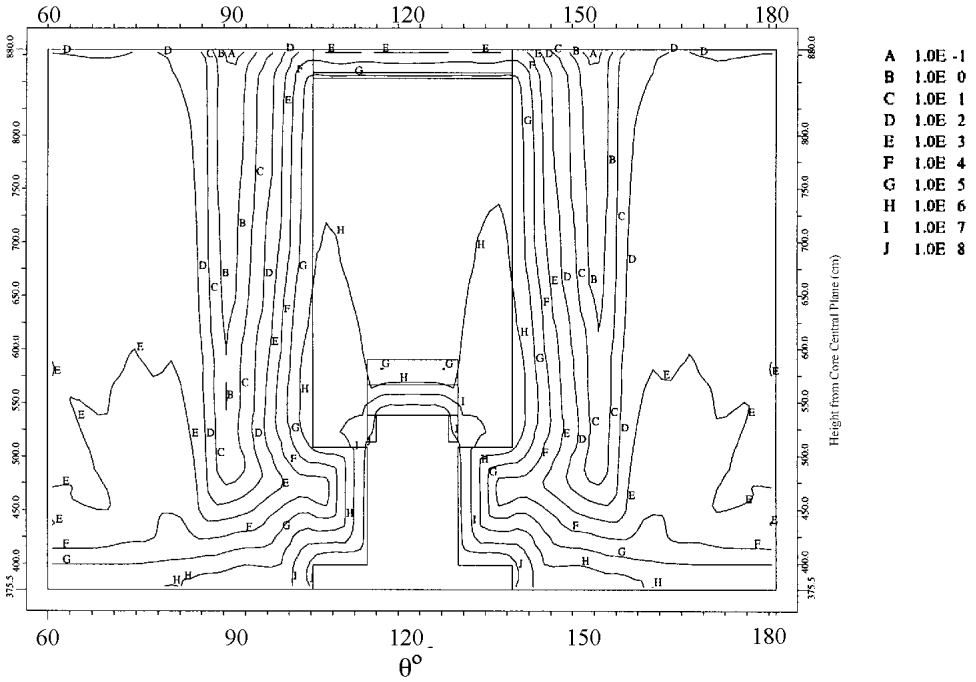

Radial distance from the Core Center= 845 cm

Fig.11 Total Neutron Flux Distribution in the Bulk Base Model (n/cm^2/s)

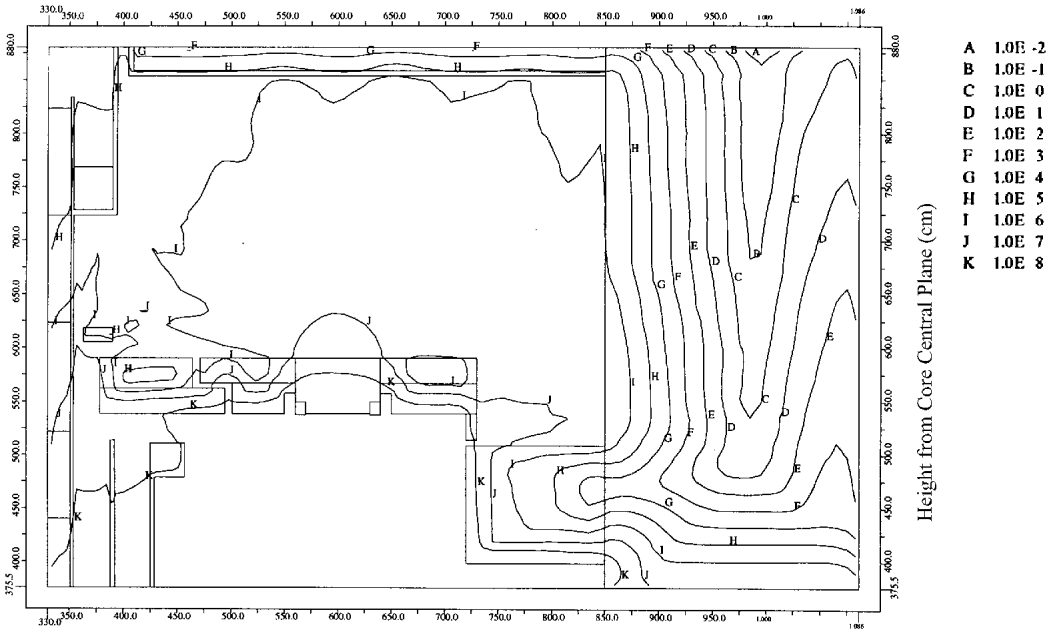

Radial distance from the Core Center (cm)

θ=135°

Fig.12 Total Neutron Flux Distribution in the Primary Coolant Inlet Piping Model (n/cm^2/s)

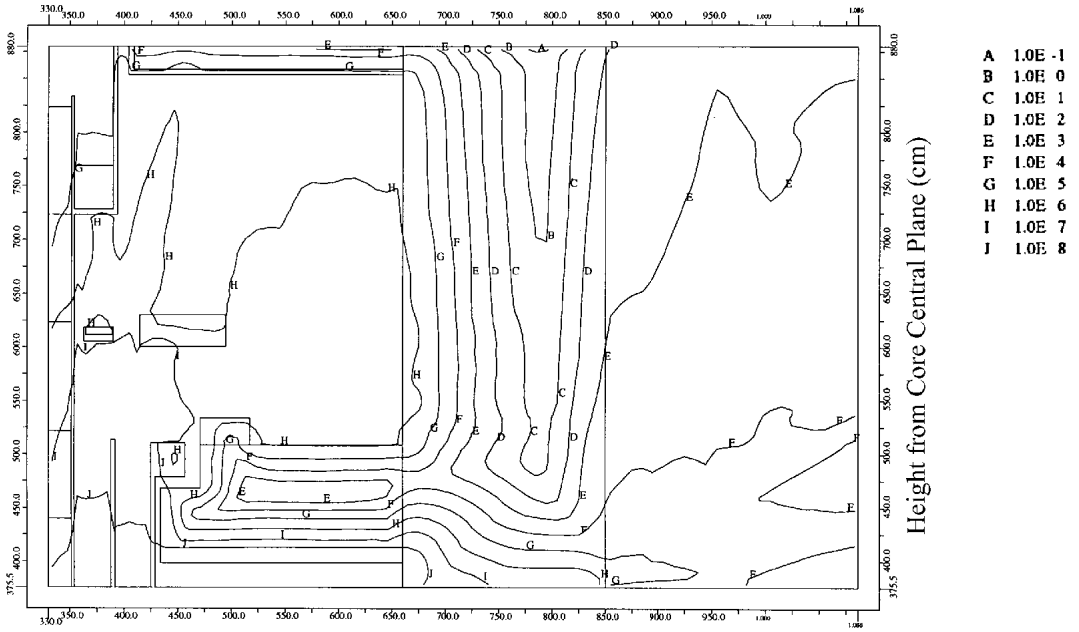

Fig.13 Total Neutron Flux Distribution in Line of the Primary Sodium Overflow Piping Model (n/cm^2/s)

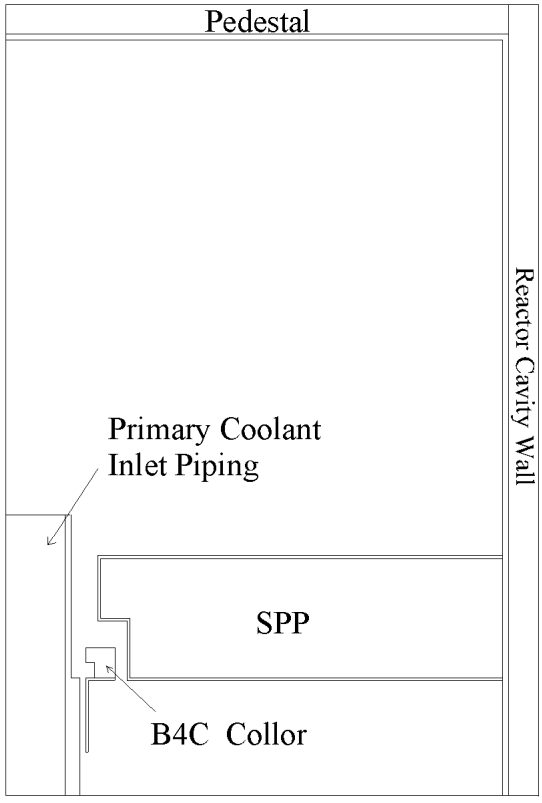

Fig.14 Design Calculation Model
(Primary Coolant Inlet Piping Model)